# Raman excitation profiles of polyatomic molecules in condensed phases. A stochastic theory

James Sue, Yi Jing Yan, and Shaul Mukamel[a)]
*Department of Chemistry, University of Rochester, Rochester, New York 14627*

(Received 6 January 1986; accepted 18 March 1986)

The absorption and the Raman excitation profiles of polyatomic molecules in condensed phases are analyzed using a stochastic model of line broadening. The electronic energy gap is assumed to be stochastically modulated by the random force resulting from the interaction with the solvent. The model interpolates all the way from homogeneous broadening (fast modulation) to inhomogeneous broadening (slow modulation). We analyze the conditions whereby the Raman excitation profiles can be expressed as the square of an ensemble-averaged amplitude. An efficient procedure for modeling both absorption and excitation profiles and extracting the relevant structural and dynamical information for large polyatomic molecules is proposed. Application is made to the Raman profiles of azulene in $CS_2$ and in methanol, and the magnitude and the inverse correlation time of the random force are extracted from the experimental data in both cases.

## I. INTRODUCTION

There is currently a considerable interest in extracting useful structural and dynamical information on complex molecular systems from Raman excitation profiles.[1-22] Some of the systems extensively studied are conjugated polyenes, aromatic molecules, and molecules of biological interest, such as porphyrins and $\beta$ carotenes in solution. The Raman process is illustrated in Fig. 1. A molecule initially in the vibronic state $|a\rangle$ and energy $\epsilon_a$ absorbs a photon $\omega_L$ and emits a photon $\omega_S$, and ends up in the vibronic state $|c\rangle$ with energy $\epsilon_c$. $|b\rangle$ and $|b'\rangle$ denote a manifold of vibronic states belonging to an excited electronic state $|e\rangle$, whereas $|a\rangle$ and $|c\rangle$ are vibronic states belonging to the ground electronic state $|g\rangle$. For isolated molecules (e.g., in supersonic beams or in the gas phase at low pressure), the steady state rate of emission of $\omega_S$ photons is given by the Kramers–Heisenberg expression[23]:

$$I_O(\omega_L,\omega_S) = 2\pi\sum_{a,c} P(a)|\bar{\chi}_{ca}(\omega_L)|^2\delta(\omega_L-\omega_S-\omega_{ca}), \tag{1}$$

where

$$\bar{\chi}_{ca}(\omega_L) = \sum_b \frac{\mu_{cb}\mu_{ba}}{\omega_L-\omega_{ba}+i\gamma_b/2} \tag{2}$$

and

$$\omega_{ij} = \epsilon_i - \epsilon_j. \tag{3}$$

Here $\epsilon_i$ is the energy of state $|i\rangle$ and $\gamma_i$ is its inverse lifetime, $P(a)$ is the equilibrium population of $|a\rangle$, $\bar{\chi}_{ca}(\omega)$ is the Raman amplitude, and $\mu_{ij}$ is the dipole matrix element between states $|i\rangle$ and $|j\rangle$.

The absorption line shape is given by the Fermi Golden Rule

$$\sigma(\omega_L) = \sum_{a,b} P(a)|\mu_{ba}|^2 \frac{\gamma_b}{(\omega_L-\omega_{ba})^2+(\gamma_b/2)^2}. \tag{4}$$

The situation is more complicated, however, for Raman spectra in condensed phases (solutions, matrices, molecular crystals, glasses, chromophores on proteins). In these cases, the molecule is subject to a random force, resulting from its interaction with a macroscopic number of external degrees of freedom, which constitute a thermal bath. The random force results in significant line broadening and loss of much of the structure in these spectra. Typically, it is possible to distinguish between two types of contributions to the emission spectra in the gas phase at finite pressure or in condensed phases.[24-34] These are denoted as Raman and fluorescence, respectively. The fluorescence component is sometimes referred to as hot luminescence or redistribution. The Raman components are relatively narrow emission lines

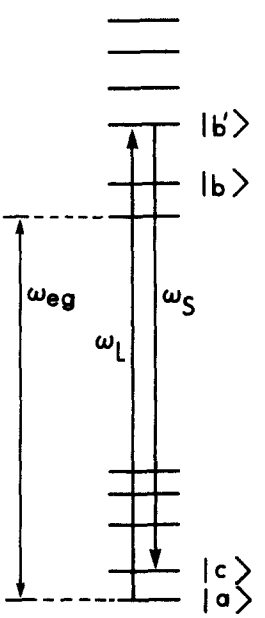


FIG. 1. The level scheme for a Raman process. $|a\rangle$ and $|c\rangle$ are vibronic states corresponding to the ground electronic state $|g\rangle$. $|b\rangle$ and $|b'\rangle$ are vibronic states corresponding to the excited electronic state $|e\rangle$. $\omega_{eg}$ is the fundamental (0–0) transition frequency.

[a)] Camille and Henry Dreyfus Teacher–Scholar.

 0021-9606/86/130462-13$02.10 © 1986 American Institute of Physics

Downloaded 26 Jun 2002 to 128.151.176.185. Redistribution subject to AIP license or copyright, see http://ojps.aip.org/jcpo/jcpcr.jsp

occurring at $\omega_L - \omega_S = \omega_{ca}$ where $|a\rangle$ and $|c\rangle$ are any pair of ground state vibronic levels, and their widths are a few $cm^{-1}$. The fluorescence lines are much broader (typical width of a few hundred $cm^{-1}$), and their maxima occur at $\omega_s = \omega_{bc}$, where levels $|b\rangle$ and $|c\rangle$ belong to the excited and the ground electronic states, respectively. A clear distinction between these two components may be made by tuning $\omega_L$ across the absorption spectrum. The Raman lines which occur at a fixed $\omega_L - \omega_S$ will follow the tuning of $\omega_L$, whereas the fluorescence components will remain roughly in the same positions.[26,32]

In the presence of an external bath, the Kramers–Heisenberg expression [Eqs. (1) and (2)], and Eq. (4) for the absorption, no longer hold, and a more general theoretical approach is needed. A microscopic theory was developed recently[20] which allows the calculation of both the Raman and the fluorescence components of a polyatomic molecule in solution. The theory starts with the density matrix (in contrast to the Kramers–Heisenberg formula which is based on the wave function) and results in a formal expression for $I(\omega_L,\omega_S)$ in terms of a four-point correlation function of the dipole operator.[20–22] The latter was then evaluated using a stochastic Langevin model for the solvent. This stochastic model was used by Kotani and Toyozawa,[33] and by Takagahara, Hanamura, and Kubo[34] for the luminescence spectra of impurities in solids. The rate of emission of $\omega_S$ photons is partitioned as

$$I(\omega_L,\omega_S) = I_R(\omega_L,\omega_S) + I_F(\omega_L,\omega_S), \tag{5}$$

where $I_R$ and $I_F$ represent the Raman and the fluorescence components, respectively. $I_R$ assumes the form

$$I_R(\omega_L,\omega_S) = 2\pi\sum_{a,c} P(a) I_{ca}(\omega_L)\delta(\omega_L - \omega_S - \omega_{ca}), \tag{6}$$

where $I_{ca}(\omega_L)$ is the Raman excitation profile for the $ca$ transition. The precise conditions for distinguishing between these components will be analyzed in Sec. II. There are three types of experimental observables in a molecular Raman experiment: (i) the absorption spectrum, $\sigma(\omega_L)$; (ii) the excitation profiles, $I_{ca}(\omega_L)$, obtained by tuning $\omega_L$ and detecting the narrow Raman component at $\omega_S = \omega_L - \omega_{ca}$; each pair of ground vibronic states $|a\rangle$ and $|c\rangle$ has its distinct excitation profile; (iii) the fluorescence spectrum, $I_F(\omega_L,\omega_S)$.

In this article we develop a simple and efficient scheme for computing $\sigma(\omega_L)$ and $I_{ca}(\omega_L)$ for large polyatomic molecules in solution. $I_F(\omega_L,\omega_S)$ contains extremely useful information as well but its calculation is more complex, and it will be analyzed in a separate article.[35] In Sec. II we present the stochastic model for line broadening which interpolates between the fast modulation (homogeneous) and the static (inhomogeneous) limits, and calculate the absorption line shape for a polyatomic molecule in solution using this broadening model. In Sec. III we derive the expression for the Raman excitation profiles. We show that when the rapid fluctuation limit holds (i.e., when the bath motions are rapid compared with the Raman linewidth), we can express the Raman components as the square of an ensemble-averaged amplitude which we denote by $\chi_{ca}(\omega_L)$. This limit is expected to hold in solution and allows us to calculate the Raman line shapes very conveniently. In Sec. IV we specialize to harmonic molecules for which the expression for the ensemble-averaged Raman amplitude $\chi_{ca}(\omega_L)$ can be greatly simplified and may be recast in an "eigenstate-free" form. In this case the necessary summations over intermediate states can be carried out analytically resulting in a simple expression most suitable for numerical computation. Our formula generalizes the existing inversion procedures commonly used in the interpretation of Raman line shapes[1–3,10,36] since it involves a more general broadening with an arbitrary time scale of the bath, and does not require perturbation theory in the displacements of the equilibrium positions. In Sec. V we apply these results to the Raman line shapes of azulene in $CS_2$ and in methanol and evaluate the magnitude and the correlation time of the random force from the experimental data. Finally, Sec. VI contains some conclusions and discussion.

## II. THE ABSORPTION LINE SHAPE FOR THE STOCHASTIC MODEL

In this section we present our general stochastic model for the Raman line shapes of polyatomic molecules in condensed phases[20] and analyze the absorption line shape. This is a unified model which interpolates continuously between homogeneous (Lorentzian) and inhomogeneous (Gaussian) line broadening.

We consider a molecule with two electronic states, the ground state $|g\rangle$ and an excited state $|e\rangle$. The molecular Hamiltonian is

$$H = |g\rangle H_g\langle g| + |e\rangle[H_e + \omega_{eg} - (i/2)\gamma]\langle e|. \tag{7}$$

Here $\gamma$ is the inverse lifetime of the electronic excited state and $\omega_{eg}$ is the electronic energy gap (0–0 transition) between the two states. For an isolated molecule $\omega_{eg}$ is simply a constant. We shall assume, however, that due to the random force exerted on the molecule by the solvent, $\omega_{eg}$ becomes a stochastic function of time, i.e.,

$$\omega_{eg} = \bar{\omega}_{eg} + \delta\omega_{eg}(t), \tag{8}$$

where $\bar{\omega}_{eg}$ is the mean electronic energy gap. $\delta\omega_{eg}(t)$ is taken to be a Gaussian–Markovian process with zero mean

$$\langle\delta\omega_{eg}(t)\rangle = 0, \tag{9a}$$

and its correlation function is

$$\langle\delta\omega_{eg}(t)\delta\omega_{eg}(0)\rangle = \Delta^2\exp(-\Lambda t). \tag{9b}$$

Here $\langle\ldots\rangle$ denotes averaging over the stochastic variables. $\Delta$ is the *amplitude* of the modulation, and $\Lambda^{-1}$ is its time scale (*correlation time*). The states $|a\rangle$, $|c\rangle$, etc. (Fig. 1) are the vibronic eigenstates of $H_g$,

$$H_g|i\rangle = \epsilon_i|i\rangle, \quad i = a, c, \ldots, \tag{10}$$

whereas the states $|b\rangle$, $|b'\rangle$ are the vibronic eigenstates of $H_e$, i.e.,

$$(\bar{\omega}_{eg} + H_e)|i\rangle = \epsilon_i|i\rangle, \quad i = b, b', \ldots. \tag{11}$$

We shall now analyze the absorption spectrum of our model system. The absorption line shape for a two-level system undergoing the same line broadening process is well known,[37–39] and the extension to our multilevel system is



Downloaded 26 Jun 2002 to 128.151.176.185. Redistribution subject to AIP license or copyright, see http://ojps.aip.org/jcpo/jcpcr.jsp

straightforward. Equation (4) then becomes[20,34,39]

$$\sigma(\omega_L) = 2\pi \sum_{a,b} P(a)|\mu_{ba}|^2 \sigma_{ba}(\omega_L), \tag{12}$$

where $\sigma_{ba}(\omega_L)$ is the contribution of the $ab$ transition to the line shape

$$\sigma_{ba}(\omega_L) = -1/\pi \,\mathrm{Im}\, J_0(\omega_L - \omega_{ba} + i\gamma/2). \tag{13}$$

The line shape function $J_0(s)$ is given by

$$J_0(s) = -i\int_0^\infty d\tau \exp[is\tau - g(\tau)], \tag{14}$$

where

$$g(\tau) = \int_0^\tau d\tau_1 \int_0^{\tau_1} d\tau_2 \langle \delta\omega_{eg}(\tau_2)\delta\omega_{eg}(0)\rangle. \tag{15}$$

Upon the substitution of Eq. (9) in Eq. (15), we get

$$g(\tau) = \frac{\Delta^2}{\Lambda^2}[\exp(-\Lambda\tau) - 1 + \Lambda\tau]. \tag{16}$$

It is possible to derive a continued fraction expression for $J_0(s)$.[20,34,39] To that end, we introduce the following set of auxiliary functions:

$$J_n(s) = -i\int_0^\infty d\tau[1 - \exp(-\Lambda\tau)]^n \exp[is\tau - g(\tau)]. \tag{17}$$

Using Eq. (17), we may derive the following recurrence relations:

$$i\left(\frac{\Delta^2}{\Lambda}\right)J_1(s) = 1 - sJ_0(s) \tag{18a}$$

and

$$(\Delta^2/\Lambda)J_{n+1}(s) = n\Lambda J_{n-1}(s) + (is - n\Lambda)J_n(s), \quad n = 1,2\ldots. \tag{18b}$$

Solving Eqs. (18) results in[39]

$$J_0(s) = \cfrac{1}{s - \cfrac{\Delta^2}{s + i\Lambda - \cfrac{2\Delta^2}{s + 2i\Lambda - \cfrac{3\Delta^2}{s + 3i\Lambda \ldots}}}}. \tag{19}$$

Equations (18) together with Eq. (19) allow us to calculate $J_n(s)$, $n = 1,2,\ldots$, recursively. The nature of the line shape function [Eq. (19)] depends on the dimensionless parameter

$$\kappa \equiv \frac{\Lambda}{\Delta}. \tag{20}$$

The *fast modulation* (homogeneous) limit is obtained when the correlation time of the bath fluctuations is very fast compared with their magnitude, i.e., $\kappa \gg 1$. In this case, the $\exp(-\Lambda\tau)$ in the right-hand side of Eq. (16) vanishes very rapidly and may be ignored. We then get

$$g(\tau) = \hat{\Gamma}\tau, \tag{21a}$$

where

$$\hat{\Gamma} = \frac{\Delta^2}{\Lambda}. \tag{21b}$$

Upon the substitution of Eq. (21a) in Eq. (14), we get

$$J_0(s) = \frac{1}{s + i\hat{\Gamma}}. \tag{22}$$

In this case, the absorption line shape assumes a Lorentzian form corresponding to homogeneous dephasing and Eqs. (13) and (22) result in

$$\sigma_{ba}(\omega_L) = \frac{\Gamma/\pi}{(\omega_L - \omega_{ba})^2 + \Gamma^2}, \tag{23a}$$

where

$$\Gamma = \hat{\Gamma} + \gamma/2. \tag{23b}$$

The *slow modulation* (static, inhomogeneous) limit is obtained when $\Lambda \ll \Delta$, i.e., $\kappa \ll 1$. In this case, we can make a Taylor expansion of Eq. (16) (short-time approximation) resulting in

$$g(\tau) = \frac{\Delta^2\tau^2}{2}. \tag{24}$$

The absorption line shape [Eq. (13)] assumes in this case the Voigt profile (a convolution of a Gaussian and a Lorentzian)

$$\sigma_{ba}(\omega_L) = \frac{1}{\sqrt{2\pi}\Delta}\int d\omega' \frac{\gamma/2\pi}{(\omega_L - \omega_{ba} - \omega')^2 + \gamma^2/4} \times \exp\left[\frac{-\omega'^2}{2\Delta^2}\right] \tag{25}$$

and when $\gamma \ll \Delta$, it becomes a Gaussian:

$$\sigma_{ba}(\omega_L) = \frac{1}{\sqrt{2\pi}\Delta}\exp\left[\frac{-(\omega_L - \omega_{ba})^2}{2\Delta^2}\right]. \tag{26}$$

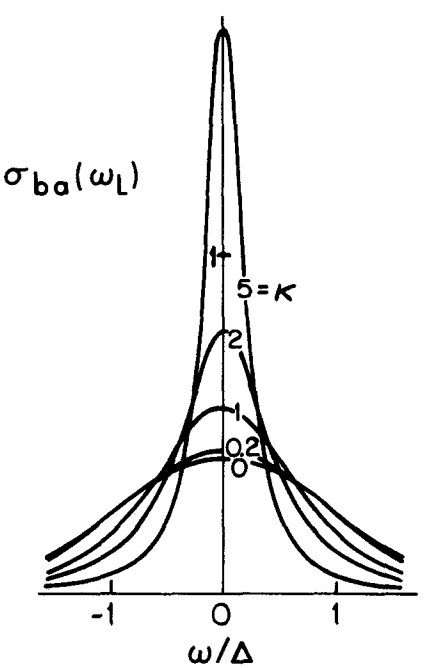


FIG. 2. The absorption line shape function [Eq. (13)] for a two-level system with a stochastic modulation [Refs. 20, 29, 37–39]. The parameter $\kappa \equiv \Lambda/\Delta$ determines the nature of the modulation. $\kappa \gg 1$ corresponds to a homogeneous broadening (a Lorentzian line shape), whereas $\kappa \ll 1$ corresponds to static inhomogeneous broadening (a Gaussian line shape). $\gamma = 0$.



Downloaded 26 Jun 2002 to 128.151.176.185. Redistribution subject to AIP license or copyright, see http://ojps.aip.org/jcpo/jcpcr.jsp

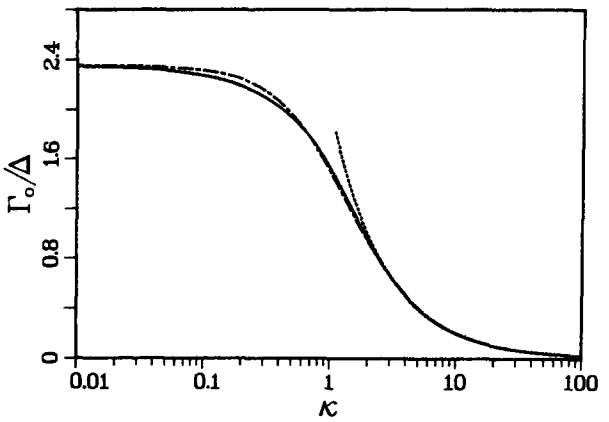


FIG. 3. The full-width at half-maximum ($\Gamma_0/\Delta$) of the stochastic line shape function $\sigma_{ba}(\omega_L)$ [Eq. (13)] vs $\kappa$, $\gamma = 0$. Solid line—exact curve (calculated numerically); dot–dashed line—the Padé approximant Eq. (27); dotted line—$\Gamma_0/\Delta = 2/\kappa$, which holds in the fast modulation limit when $\kappa \gg 1$ [Eq. (21b)].

As $\kappa$ is varied, the absorption line shape thus changes continuously from a Gaussian to a Lorentzian. This is illustrated in Fig. 2, in which we have plotted $\sigma_{ba}(\omega_L)$ for various values of $\kappa$. We shall denote the full-width at half-maximum of the absorption line shape $\sigma_{ba}(\omega_L)$ [Eq. (13) with $\gamma = 0$] by $\Gamma_0$. We have found it useful in our subsequent analysis to express $\Gamma_0$ in terms of the stochastic parameters $\Delta$ and $\Lambda$. In the fast modulation limit $\Gamma_0 = 2\hat{\Gamma} = 2\Delta^2/\Lambda$ whereas in the slow modulation limit $\Gamma_0 = 2.355\ \Delta$. In Fig. 3 we display $\Gamma_0/\Delta$ vs $\kappa$. This curve can be adequately represented by the Padé approximant:

$$\frac{\Gamma_0}{\Delta} = \frac{2.355 + 1.76\kappa}{1 + 0.85\kappa + 0.88\kappa^2}. \tag{27}$$

This approximant is plotted in Fig. 3 as well, and it is good to within 3%.

## III. THE RAMAN EXCITATION PROFILES

In a stationary Raman experiment the molecule is irradiated with a monochromatic radiation field with frequency $\omega_L$ and the steady state rate of emission of photons with frequency $\omega_S$ [$I(\omega_L,\omega_S)$] is detected. $I(\omega_L,\omega_S)$ can in general be expressed in terms of a four-point correlation function of the dipole operator which was evaluated for the present stochastic model in Ref. 20. We shall rearrange that result in the form (see Appendix A)

$$I(\omega_L,\omega_S) = I_1 + I_2 + I_3 + I_4, \tag{28a}$$

where

$$I_1 = 2\pi \sum_{a,c} P(a) |\chi_{ca}(\omega_L)|^2 \delta(\omega_L - \omega_S - \omega_{ca}), \tag{28b}$$

$$I_2 = \sum_{a,c} P(a) \sum_{n=1}^{\infty} \frac{1}{n!} \chi_{ca}^{(n)}(\omega_L)\, \chi_{ca}^{(n)*}(\omega_S + \omega_{ca}) \times \frac{n\Lambda}{(\omega_L - \omega_S - \omega_{ca})^2 + (n\Lambda)^2} + \text{c.c.}, \tag{28c}$$

$$I_3 = -i \sum_{a,c} P(a) \sum_{b,b'} \mu_{ab'}\mu_{b'c}\mu_{cb}\mu_{ba} \sum_{n=0}^{\infty} \frac{1}{\kappa^{2n} n!} J_n(\omega_L - \omega_{ba} + i\gamma/2) \times \left\{ \frac{(-1)^n J_n(\omega_S - \omega_{bc} + i\gamma/2) + J_n(\omega_{b'c} - \omega_S + i\gamma/2)}{\omega_{b'b} + i(\gamma + n\Lambda)} \right\} + \text{c.c.}, \tag{28d}$$

and

$$I_4 = i \sum_{a,c} P(a) \sum_{n=0}^{\infty} \frac{1}{n!} \chi_{ca}^{(n)}(\omega_L) \chi_{ca}^{(n)*}(\omega_S + \omega_{ca}) \times \frac{\omega_L - \omega_S - \omega_{ca}}{(\omega_L - \omega_S - \omega_{ca})^2 + (n\Lambda)^2} + \text{c.c.} \tag{28e}$$

Here the Raman amplitudes $\chi_{ca}^{(n)}(\omega)$ are defined as

$$\chi_{ca}^{(n)}(\omega) = \frac{1}{\kappa^n} \sum_b \mu_{cb}\mu_{ba} J_n(\omega - \omega_{ba} + i\gamma/2) \tag{29a}$$

and

$$\chi_{ca}(\omega) \equiv \chi_{ca}^{(0)}(\omega) = \sum_b \mu_{cb}\mu_{ba} J_0(\omega - \omega_{ba} + i\gamma/2). \tag{29b}$$

We shall now explore the partitioning of $I(\omega_L,\omega_S)$ [Eq. (28)] into a Raman and a fluorescence component [Eq. (5)]. As already indicated in the Introduction, such a distinction can be made when the emission spectrum consists of relatively narrow lines centered around $\omega_L - \omega_S = \omega_{ca}$, where $|c\rangle$ and $|a\rangle$ are two ground state vibronic levels, and a much broader emission which does not vary considerably as we tune $\omega_L$. When this situation holds, we denote the former lines as Raman and the latter broad emission as fluorescence. It is clear from Eq. (28) that $I_1$ represents a Raman component, whereas $I_3$ and $I_4$ definitely belong to the fluorescence, as they do not show any resonant behavior at $\omega_L - \omega_S = \omega_{ca}$. The classification $I_2$ as Raman or fluorescence is more subtle and depends on the broadening parameters, in particular the value of $\Lambda^{-1}$, the solvent time scale. We shall, therefore, distinguish now between several cases.

### A. The isolated molecule limit

In the absence of a thermal bath, Eq. (28) reduces to the Kramers–Heisenberg formula [Eq. (1)], and the entire emission can be viewed as Raman (no fluorescence component). This is obtained as follows: as we switch off the bath by letting the modulation amplitude $\Delta \to 0$, we have $\kappa \to \infty$. As a result, we can neglect all the terms in Eq. (28) with $n > 0$, since they contain a $\kappa^{-2n}$ factor, and keep only $n = 0$.



Downloaded 26 Jun 2002 to 128.151.176.185. Redistribution subject to AIP license or copyright, see http://ojps.aip.org/jcpo/jcpcr.jsp

Consequently, $I_2 = 0$. In addition, an interference occurs between $I_3$ and $I_4$ in this case, and they exactly cancel, $I_3 + I_4 = 0$ [see. Eq. (37a)]. We then get

$$I_F(\omega_L,\omega_S) = I_2 + I_3 + I_4 = 0, \tag{30a}$$

$$I_R(\omega_L,\omega_S) = I_1, \tag{30b}$$

i.e.,

$$I_R(\omega_L,\omega_S) = 2\pi\sum_{a,c} P(a)|\chi_{ca}(\omega_L)|^2\delta(\omega_L - \omega_S - \omega_{ca}) \tag{31}$$

and $\chi_{ca}(\omega)$ is given by Eq. (29b), which is identical in this case to $\chi_{ca}(\omega)$ [Eq. (2)]. The entire emission, in this case, is of the Raman-type and is given by the Kramers–Heisenberg formula [Eq. (1)].

### B. The rapid fluctuation limit

The Raman components of the $I_1$ term are proportional to $\delta(\omega_L - \omega_S - \omega_{ca})$ and have a zero width within our model. Had we included a finite lifetime for the ground state levels $|a\rangle$ and $|c\rangle$ ($\gamma_a^{-1}$ and $\gamma_c^{-1}$, respectively), the Raman component would acquire a finite width, with FWHM equal to $\gamma_a + \gamma_c$. The rapid fluctuation limit is defined by the condition

$$\Lambda \gg \gamma_a + \gamma_c. \tag{32}$$

This limit should not be mixed with the fast modulation limit [case (c)] where $\kappa \equiv \Lambda/\Delta \gg 1$. Here we merely require the bath time scale $\Lambda^{-1}$ to be short compared with the lifetimes of levels $|a\rangle$ and $|c\rangle$, and $\kappa$ can be arbitrarily small or large. When condition (32) holds, the emission lines of $I_2$ (whose widths are $n\Lambda$, $n = 1,2,...$) are much broader than the "Raman" lines of $I_1$, and $I_2$ naturally contributes to the broad fluorescence rather than to the narrow Raman components. We therefore have in this case

$$I_F(\omega_L,\omega_S) = I_2 + I_3 + I_4, \tag{33a}$$

$$I_R(\omega_L,\omega_S) = I_1, \tag{33b}$$

i.e.,

$$I_R(\omega_L,\omega_S) = 2\pi\sum_{a,c} P(a)|\chi_{ca}(\omega_L)|^2\delta(\omega_L - \omega_S - \omega_{ca}) \tag{34a}$$

with

$$\chi_{ca}(\omega_L) = \sum_b \mu_{cb} J_0(\omega_L - \omega_{ba} + i\gamma/2)\mu_{ba} \tag{34b}$$

or alternatively

$$\chi_{ca}(\omega_L) = -i\sum_b \mu_{cb}\mu_{ba}\int_0^\infty d\tau \exp[i(\omega_L - \omega_{ba})\tau - (\gamma/2)\tau - g(\tau)]. \tag{34c}$$

Equation (34) is an extremely important result. It shows that the Raman spectrum in the rapid fluctuation limit can be expressed in terms of an ensemble-averaged amplitude $\chi_{ca}(\omega)$. This limit usually holds for polyatomic molecules in solutions. In this respect Eq. (34) is similar to the Kramers–Heisenberg formula [Eq. (1)]. It should be emphasized, however, that Eq. (34) is more general and corresponds to a reduced description of the Raman process in which the effects of the thermal bath are properly incorporated by the line broadening function $g(\tau)$. The Kramers–Heisenberg formula is recovered only if we set $g(\tau) = 0$ in Eq. (34c), and $\chi_{ca}(\omega_L)$ then assumes a simple Lorentzian form [Eq. (2)]. Furthermore our analysis shows that Eq. (34a) gives only the Raman component and cannot reproduce the entire emission spectrum which includes the fluorescence component as well. Several recent theoretical studies of Raman line shapes of polyatomic molecules in solution had started with the Kramers–Heisenberg formula, taking it for granted that the Raman process can be expressed in terms of an ensemble-averaged amplitude. The amplitude was then successfully adjusted to account for the Raman excitation profiles.[1,2,5–8] Our present derivation of Eq. (34a) shows that this success stems from the fact that in the *rapid fluctuation* limit a Kramers–Heisenberg-type formula is valid and the Raman process can be described by an ensemble-averaged amplitude. Our numerical calculations in Sec. V for azulene in $CS_2$ and in methanol show that the rapid fluctuation limit typically holds for polyatomic molecules in solution.

### C. The fast modulation (homogeneous) limit

This limit is obtained when

$$\kappa \equiv \Lambda/\Delta \gg 1. \tag{35}$$

In this case the bath time scale $\Lambda^{-1}$ is very fast compared with the amplitude of modulation $\Delta$. All the terms in Eq. (28) with $n > 0$ are negligible since they contain a $\kappa^{-2n}$ factor. We further have [Eq. (22)]

$$J_0(\omega + i\gamma/2) = \frac{1}{\omega + i\hat{\Gamma}}, \tag{36a}$$

where

$$\Gamma = \gamma/2 + \hat{\Gamma} \tag{36b}$$

and

$$\hat{\Gamma} = \frac{\Delta^2}{\Lambda}. \tag{36c}$$

Upon the substitution of Eq. (36) in Eq. (28) and retaining only the terms with $n = 0$ we get

$$I_F(\omega_L,\omega_S) = I_3 + I_4 = 2\hat{\Gamma}\sum_{a,c} P(a)\sum_{b,b'} \mu_{ab'}\mu_{b'c}\mu_{cb}\mu_{ba} \times \frac{1}{\omega_L - \omega_{ba} + i\Gamma}\frac{1}{\omega_L - \omega_{b'a} - i\Gamma} \times \frac{1}{\omega_{b'b} + i\gamma}\frac{1}{\omega_{bc} - \omega_S - i\Gamma} + \text{c.c.}, \tag{37a}$$

and

$$I_R(\omega_L,\omega_S) = I_1 = 2\pi\sum_{a,c} P(a)|\chi_{ca}(\omega_L)|^2\delta(\omega_L - \omega_S - \omega_{ca}) \tag{37b}$$

with

$$\chi_{ca}(\omega_L) = \sum_b \mu_{cb}\mu_{ba}\frac{1}{\omega_L - \omega_{ba} + i\Gamma}. \tag{37c}$$



Downloaded 26 Jun 2002 to 128.151.176.185. Redistribution subject to AIP license or copyright, see http://ojps.aip.org/jcpo/jcpcr.jsp

Equation (37a) shows that $I_F(\omega_L,\omega_S)$ is induced by the bath. In the absence of broadening ($\Gamma = 0$), $I_F(\omega_L,\omega_S)$ vanishes due to the interference between $I_3$ and $I_4$ and the entire emission is of the Raman-type. We then recover the isolated molecule limit [Eqs. (30) and (31)]. It should be noted also that Eq. (37c) is a limiting form of Eq. (34b) when $J_0(s)$ assumes a Lorentzian form.

### D. The static (inhomogeneous) limit

In the static limit, the bath is infinitely slow, so that $\Lambda = 0$ and $\kappa = 0$. In this case, the interference between $I_3$ and $I_4$ occurs in the same way as for the isolated molecule, and $I_3 + I_4 = 0$. Regarding $I_2$, we note that when $\Lambda = 0$ we have

$$\frac{n\Lambda}{(\omega_L - \omega_S - \omega_{ca})^2 + (n\Lambda)^2} = \pi\delta(\omega_L - \omega_S - \omega_{ca}). \tag{38}$$

Therefore, $I_2$ contributes to the Raman component as well, and we have

$$I_F(\omega_L,\omega_S) = I_3 + I_4 = 0, \tag{39a}$$

$$I_R(\omega_L,\omega_S) = I_1 + I_2, \tag{39b}$$

i.e.,

$$I_R(\omega_L,\omega_S) = 2\pi\sum_{a,c}P(a)\sum_{n=0}^{\infty}\frac{1}{n!}|\chi_{ca}^{(n)}(\omega_L)|^2 \times\delta(\omega_L - \omega_S - \omega_{ca}), \tag{40a}$$

where $\chi_{ca}^{(n)}$ is given by Eq. (29), i.e.,

$$\chi_{ca}^{(n)}(\omega_L) = -i\sum_b \mu_{cb}\mu_{ba}\int_0^{\infty} d\tau(\Delta\tau)^n \times\exp[i(\omega_L - \omega_{ba})\tau - (\gamma/2)\tau - \Delta^2\tau^2/2]. \tag{40b}$$

The summation over $n$ in Eq. (40a) can now be carried out (see Appendix B), resulting in

$$I_R(\omega_L,\omega_S) = \frac{1}{\sqrt{2\pi}\Delta}\int_{-\infty}^{\infty} d\omega' \exp\left(\frac{-\omega'^2}{2\Delta^2}\right) \times I_0(\omega_L - \omega',\omega_S - \omega'), \tag{41}$$

where $I_0(\omega_L,\omega_S)$ [Eq. (1)] is the Raman spectrum of the isolated molecule. Equation (41) is the well-known result for inhomogeneous broadening. In this case we can calculate the emission spectrum for a particular realization of the energy gap using the Kramers–Heisenberg formula, resulting in $I_0(\omega_L,\omega_S)$. We then average the result over the static distribution of the electronic energy gap.

### E. Raman spectra at large detunings

When the incident frequency $\omega_L$ is tuned way off resonance from any molecular frequency $\omega_{ba}$, the general expression for the Raman line shape simplifies considerably. Let us assume that for any pair of levels $|a\rangle$ and $|b\rangle$ we have

$$|\omega_L - \omega_{ba}| \gg \Delta,\Lambda. \tag{42}$$

Condition (42) also implies that $|\omega_L - \omega_{ba}| \gg \Gamma_0$ where $\Gamma_0$ is the FWHM of the absorption line shape $\sigma_{ba}(\omega_L)$ (see Fig. 3). (Note that $\Gamma_0 \leqslant 2.355\Delta$). In this case, $\chi_{ca}^{(n)}(\omega)$ are flat and do not vary significantly when $\omega_L$ is detuned by a few $\Gamma_0$. We can then substitute in Eq. (28c)

$$\chi_{ca}^{(n)}(\omega_S + \omega_{ca}) \approx \chi_{ca}^{(n)}(\omega_L), \tag{43}$$

resulting in

$$I_R(\omega_L,\omega_S) = I_1 + I_2 \approx 2\pi\sum_{a,c}P(a)\sum_{n=0}^{\infty}\frac{1}{n!}|\chi_{ca}^{(n)}(\omega_L)|^2 \times\frac{n\Lambda/\pi}{(\omega_L - \omega_S - \omega_{ca})^2 + (n\Lambda)^2}. \tag{44}$$

Equation (44) becomes exact in the static limit, when $\Lambda = 0$, irrespective of the magnitude of $\Gamma_0$, and reduces to Eq. (40a). Making use of Eq. (17) we can develop an asymptotic expansion for $J_n(s)$ for large $s$ (by considering the short time behavior of the integrand). The leading term (lowest order in $1/s$) is

$$J_n(s) \sim \frac{(i\Lambda)^n n!}{s^{n+1}} \tag{45}$$

which holds for $|s| \gg \Delta,\Lambda$. Upon the substitution of Eq. (45) together with Eq. (29) into Eq. (44), we note that when Eq. (42) holds we can neglect all the terms in Eq. (44) with $n > 0$ and retain only those with $n = 0$. Under these conditions, $I_3 + I_4$ interfere destructively and cancel (in the same way as for the isolated molecule), and we finally get

$$I_F(\omega_L,\omega_S) = I_3 + I_4 \approx 0, \tag{46a}$$

$$I_R(\omega_L,\omega_S) = I_1 \approx 2\pi\sum_{a,c}P(a)|\chi_{ca}(\omega_L)|^2\delta(\omega_L - \omega_S - \omega_{ca}), \tag{46b}$$

where $\chi_{ca}(\omega)$ is given by Eq. (2) and does not contain any broadening due to the interaction with the solvent. Equation (44), in this case, reduces to the Kramers–Heisenberg formula, and we see only the Raman component. Equations (42)–(46) imply that for large detunings the effect of the thermal bath becomes negligible, and the molecule behaves as an isolated molecule. The reason is that at large detunings, the Raman scattering process is very rapid [time scale $\sim(\omega_L - \omega_{ba})^{-1}$] and the bath does not have time to affect the process. It should be noted that when $\gamma \gg \Delta,\Lambda$, then $|s| = |\omega + i\gamma/2| \gg \Delta,\Lambda$, and the line broadening is always dominated by the inverse lifetime $\gamma$ and the effects of the bath are negligible so that Eq. (46b), the Kramers–Heisenberg expression is recovered for any detuning.

In concluding this section we note that depending on the nature of the line broadening, the Raman excitation profiles are given by Eqs. (31) or Eq. (34a) or Eq. (37b) or Eq. (41) or Eq. (46b). In all cases the calculation requires the amplitude $\chi_{ca}^{(n)}(\omega_L)$ [Eqs. (29)]. A detailed calculation for the azulene molecule will be presented in Sec. V. It should be further noted that the variation of the fluorescence intensity $I_F(\omega_L,\omega_S)$ with detuning provides a convenient means for evaluating $\Delta$ and $\Lambda$. This together with the absorption and the Raman profiles should allow an accurate estimate of these bath line broadening parameters from the experimental line shapes. We shall examine this issue in detail in a subsequent article[35] which will focus on the absolute intensity of the Raman and the fluorescence components, and on the fluorescence line shape $I_F(\omega_L,\omega_S)$.



Downloaded 26 Jun 2002 to 128.151.176.185. Redistribution subject to AIP license or copyright, see http://ojps.aip.org/jcpo/jcpcr.jsp

## IV. RAMAN EXCITATION PROFILES OF HARMONIC MOLECULES; AN EIGENSTATE-FREE PROCEDURE

In the previous sections we had derived closed expressions for the absorption, the Raman, and the fluorescence line shapes of polyatomic molecules in solution. The calculations of the absorption spectrum [Eq. (12)] involves a double summation over $a$ and $b$. The calculation of each Raman amplitude $\chi_{ca}^{(n)}(\omega)$ [Eq. (29)] involves a single sum over intermediate states $b$. The calculation of the fluorescence spectrum requires the calculation of $I_3$ [Eq. (28d)] which involves summation over four indexes $a,b,b'$, and $c$. These summations can be easily carried out for small molecules with only a few relevant vibronic levels. However for large polyatomic molecules with many modes these summations become quite tedious. In this section we shall focus on the absorption and the Raman excitation profiles of harmonic polyatomic molecules in which the potential surfaces of the ground and the electronically excited states may be expanded to quadratic order in the nuclear coordinates. Using Green function techniques it is possible to perform the necessary summations over intermediate states and to obtain an eigenstate-free expression for these line shapes which involves no such summations.[40,41] These expressions are extremely useful and make the calculation of absorption and Raman profiles feasible even for very large polyatomic molecules. In this section we introduce the harmonic model and the eigenstate-free expressions which will be used in Sec. V for calculating the Raman profiles of the azulene molecule.

We consider a polyatomic harmonic molecule with $N$ vibrational modes. Its Hamiltonian is written in the form

$$H = |g\rangle H_g \langle g| + |e\rangle [H_e + \omega_{eg} - (i/2)\gamma] \langle e|, \tag{47}$$

$$H_e = \frac{1}{2}\sum_{j=1}^{N} \omega_j' (p_j'^2 + q_j'^2 - 1). \tag{48b}$$

$$H_e = \frac{1}{2}\sum_{j=1}^{N} \omega_j' (p_j'^2 + q_j'^2 - 1). \tag{48b}$$

We adopt the common spectroscopic notation, whereby we label ground state quantities by a double prime and excited state quantities by a single prime. The dimensionless momentum and coordinate corresponding to the $j$th excited state normal mode are denoted by $p_j'$ and $q_j'$, respectively:

$$p_j' = \left[\frac{1}{m_j \omega_j' \hbar}\right]^{1/2} P_j', \tag{49}$$

$$q_j' = \left[\frac{m_j \omega_j'}{\hbar}\right]^{1/2} Q_j', \tag{50}$$

$P_j'$ and $Q_j'$ being the conjugate momentum and the normal coordinate, respectively, of the $j'$th mode of the excited state. A similar transformation between $p_j''$, $q_j''$, and $P_j''$, $Q_j''$ is defined by changing all $'$ indexes in Eqs. (49) and (50) to $''$. $\omega_j'(\omega_j'')$ and $m_j$ are the frequency and the mass of the $j'$th mode, and $\omega_{eg}$ is the fundamental (0–0) transition frequency. We shall now introduce a vector notation and define the following $N$ component column vectors: $\mathbf{Q}'$, $\mathbf{Q}''$, $\mathbf{q}'$, and $\mathbf{q}''$ whose components are $Q_j'$, $Q_j''$, $q_j'$, and $q_j''$, $j = 1,\ldots,N$, respectively. The normal modes $\mathbf{Q}'$ and $\mathbf{Q}''$ are not necessarily the same, and most generally they may be related by an orthogonal transformation

$$\mathbf{Q}' = \overline{\mathbf{S}}\mathbf{Q}'' + \tilde{\mathbf{D}}, \tag{51a}$$

$$\overline{\mathbf{S}}^T \overline{\mathbf{S}} = 1, \tag{51b}$$

where $\overline{\mathbf{S}}$ is the Dushinsky transformation matrix and $\overline{\mathbf{S}}^T$ is its transpose. $\tilde{\mathbf{D}}$ is an $N$ component vector whose components $\tilde{D}_j$ denote the displacements of the equilibrium positions between the two electronic states. It will be convenient to define a new transformation matrix between the dimensionless coordinates, i.e.,

$$\mathbf{q}' = \mathbf{S}\mathbf{q}'' + \mathbf{D}, \tag{52a}$$

where $\mathbf{S}$ is related to $\overline{\mathbf{S}}$ by

$$S_{ij} = (\omega_i'/\omega_j'')^{1/2} \overline{S}_{ij}. \tag{52b}$$

$\mathbf{D}$ is the dimensionless displacement vector between the equilibrium configuration of the two electronic states. Its components $D_j$ are related to $\tilde{D}_j$ by

$$D_j = \left(\frac{m_j \omega_j'}{\hbar}\right)^{1/2} \tilde{D}_j. \tag{53}$$

Note that the matrix $\mathbf{S}$ (unlike $\overline{\mathbf{S}}$) is not orthogonal. In this section we shall introduce an additional simplifying assumption, namely, that the electronic dipole operator is weakly dependent on the nuclear coordinates, so that $\mu_{ij}$ become simply the Franck–Condon factors, i.e.,

$$\mu_{ij} = \langle i|j\rangle. \tag{54}$$

The eigenstates $|a\rangle$ and $|c\rangle$ will be denoted in this section by $|\mathbf{n}\rangle$ and $|\mathbf{m}\rangle$, respectively, i.e.,

$$|a\rangle = |\mathbf{n}\rangle = \prod_{j=1}^{N} |n_j\rangle, \tag{55a}$$

$$|c\rangle = |\mathbf{m}\rangle = \prod_{j=1}^{N} |m_j\rangle. \tag{55b}$$

The absorption line shape [Eq. (12)] is now given by

$$\sigma(\omega_L) = -2\,\mathrm{Im}\sum_{\mathbf{n}} P(\mathbf{n}) \chi_{\mathbf{nn}}(\omega_L). \tag{56}$$

The Raman excitation profiles in the rapid fluctuation limit are given by Eqs. (34) and require the calculation of $\chi_{\mathbf{mn}}(\omega)$. [The current procedure can be easily used to calculate the more general amplitudes $\chi_{\mathbf{mn}}^{(n)}(\omega)$, Eq. (29). This extension is straightforward and will not be made here explicitly]. We now need to calculate $\chi_{\mathbf{mn}}(\omega)$, where

$$\chi_{\mathbf{mn}}(\omega_L) = -i\int_0^\infty d\tau \exp[i(\omega_L + \epsilon_{\mathbf{n}})\tau] \times G_{\mathbf{mn}}(\tau)\exp[-g(\tau)] \tag{57}$$

with

$$G_{\mathbf{mn}}(\tau) = \langle \mathbf{m}|\exp(-iH_e\tau)|\mathbf{n}\rangle \tag{58}$$

and $\epsilon_{\mathbf{n}}$ is the energy of the initial state $|\mathbf{n}\rangle$. A general expression for $G_{\mathbf{mn}}(\tau)$ for the present model was derived recently.[40,41] The final result is considerably simplified when the normal modes in the ground and the excited electronic states



Downloaded 26 Jun 2002 to 128.151.176.185. Redistribution subject to AIP license or copyright, see http://ojps.aip.org/jcpo/jcpcr.jsp

are identical, i.e., when the Dushinsky transformation matrix is diagonal:

$$\bar{S}_{ij} = \delta_{ij}, \tag{59a}$$

$$S_{ij} = \lambda_{ij} = (\omega_j'/\omega_j'')^{1/2} \cdot \delta_{ij}. \tag{59b}$$

We shall therefore start with this case. We then have[41]

$$G_{\mathbf{mn}}(t) = \prod_{j=1}^{N} G_{m_j n_j}(t). \tag{60}$$

To simplify the notation, we shall, hereafter, consider a single mode and omit all the $j$ subscripts from $\omega_j'$, $\omega_j''$, $D_j$, $n_j$, and $m_j$. The total Green function can then be calculated using Eq. (60). For a single mode, we get

$$G_{mn}(t) = G_{00}(t) W_{mn}(t), \tag{61}$$

where

$$G_{00}(t) = [\psi(t)]^{-1/2} \exp[D^2 f(t)], \tag{62}$$

$$\psi(t) = \frac{(\omega_+)^2}{4\omega'\omega''} [1 - (\omega_-/\omega_+)^2 \exp(-2i\omega' t)], \tag{63a}$$

and

$$f(t) = -\frac{\omega''[1 - \exp(-i\omega' t)]}{\omega_+ - \omega_- \exp(-i\omega' t)}. \tag{63b}$$

$W_{mn}(t)$ is given by

$$W_{mn}(t) = (m!n!2^{m+n})^{-1/2} \times \sum_{p=0}^{m} \sum_{q=0}^{n} (-1)^q \binom{m}{p} \binom{n}{q} [\alpha(t)]^{m+n-p-q} \times [\tilde{\alpha}(t)]^{p+q} H_{m+n-p-q} \times [\lambda f(t) D/\alpha(t)] H_{p+q}(0) \tag{64}$$

with

$$\omega_\pm = \omega' \pm \omega'', \tag{65a}$$

$$\lambda = (\omega'/\omega'')^{1/2}, \tag{65b}$$

$$\alpha(t) = \left[\frac{1}{2} \frac{\omega_- - \omega_+ \exp(-i\omega' t)}{\omega_+ - \omega_- \exp(-i\omega' t)}\right]^{1/2}, \tag{65c}$$

$$\tilde{\alpha}(t) = \left[\frac{1}{2} \frac{\omega_- + \omega_+ \exp(-i\omega' t)}{\omega_+ + \omega_- \exp(-i\omega' t)}\right]^{1/2}. \tag{65d}$$

Here $H_n(q)$ are the Hermite polynomials. We further have

$$H_n(0) = \begin{cases} 0 & n \text{ odd} \\ (-1)^{n/2} n!/(n/2)! & n \text{ even} \end{cases}. \tag{66}$$

For supercooled molecules at zero temperature we need only $n = 0$. Equation (64) then assumes the form

$$W_{m0}(t) = (m!2^m)^{-1/2} \beta^m(t) H_m[\lambda f(t) D/\beta(t)], \tag{67a}$$

where

$$\beta(t) = [\alpha^2(t) + \tilde{\alpha}^2(t)]^{1/2} = \left\{\frac{\omega_+\omega_-[1 - \exp(-2i\omega' t)]}{\omega_+^2 - \omega_-^2 \exp(-2i\omega' t)}\right\}^{1/2}. \tag{67b}$$

For $m = 1$, i.e., for the Raman fundamental we have

$$W_{10}(t) = 2^{1/2} \lambda f(t) D. \tag{68}$$

When the frequencies $\omega'$ and $\omega''$ are the same ($\omega = \omega' = \omega''$), we have $\lambda = 1$ and $\beta(t) = 0$. Equation (67a) then reduces to the form

$$W_{m0}(t) = (m!2^m)^{-1/2} [2Df(t)]^m = (m!2^m)^{-1/2} D^m [\exp(-i\omega t) - 1]^m. \tag{69}$$

In Appendix C we present the general expression for the absorption line shape $\sigma(\omega_L)$ which incorporates the Dushinsky rotation. In Appendix D we present an expression for $G_{\mathbf{mn}}(t)$ for a special case with Dushinsky rotation. These results were used in our calculations for azulene. The most general expression for $G_{\mathbf{mn}}(t)$ is given elsewhere.[41]

## V. APPLICATION TO AZULENE

In this section, we make use of the stochastic model for harmonic molecules developed in the previous sections to calculate the absorption and the Raman excitation profiles of the 700 nm ($S_0$–$S_1$) transition of azulene.[8] The available experimental data consist of the absorption, the Raman fundamentals of the 1400, 1200, and the 900 $cm^{-1}$ modes, and the first Raman overtone of the 825 $cm^{-1}$ mode. The measurements were made at room temperature using $CS_2$ as a solvent. In addition, the absorption and the 825 $cm^{-1}$ Raman fundamental were also measured in methanol. Our calculations were made using Eqs. (34), (56), and (57). $G_{\mathbf{mn}}(t)$ were first calculated and $\chi_{\mathbf{mn}}(\omega)$ were then computed using a standard fast Fourier transform routine. We have used 8192 time points with a step size of $\Delta t = 6.4 \times 10^{-15}$ s. The ground state and the excited state seven-mode frequencies $\omega'$ and $\omega''$, were taken from Ref. 8(b) and the displacements $D_j$ and the broadening parameters ($\Delta$ and $\Lambda$) were adjusted to fit the $CS_2$ data. We first attempted to obtain the best fit without a Dushinsky rotation making use of Eqs. (60)–(66) for $G_{\mathbf{mn}}(t)$. The structural parameters of our best fit are given in Table I. The solvent line-broadening parameters of our fit are $\Delta = 180$ $cm^{-1}$, $\Lambda = 18 cm^{-1}$ corresponding to $\kappa = 0.1$ and $\Gamma_0 = 408$ $cm^{-1}$ (Fig. 3). The resulting line shapes are shown in Fig. 4. It is clear that the overall fit for the absorption and the 1400, 1260, and 825 $cm^{-1}$ modes is satisfactory. The calculated intensity of the 900 $cm^{-1}$ vibration (mode 4) is too weak, and that of 1400 $cm^{-1}$ vibration (mode 6) is too large. We therefore introduced a Dushinsky rotation parameter to couple the 1400 and 900 $cm^{-1}$ modes, keeping all other parameters fixed, and we were then able to obtain a good simultaneous fit of the absorption and all the Raman profiles. A similar procedure was used in Ref. 8(b). The resulting Dushinsky rotation parameter ($\bar{S}_{4,6} = -0.25$) is the same as that obtained in Ref. 8(b). The present theory generalizes the treatment of Ref. 8(b) in two

TABLE I. The ground state and excited state frequencies and the dimensionless displacements used in our best fit seven-mode calculation of azulene.

| Mode | 1 | 2 | 3 | 4 | 5 | 6 | 7 |
|---|---|---|---|---|---|---|---|
| $\omega_j''$ ($cm^{-1}$) | 406 | 679 | 825 | 900 | 1260 | 1400 | 1562 |
| $\omega_j'$ ($cm^{-1}$) | 384 | 662 | 857 | 900 | 1193 | 1388 | 1550 |
| $D_j$ | 0.61 | 0.76 | 1.23 | 0.55 | 0.77 | 1.09 | 1.12 |



Downloaded 26 Jun 2002 to 128.151.176.185. Redistribution subject to AIP license or copyright, see http://ojps.aip.org/jcpo/jcpcr.jsp

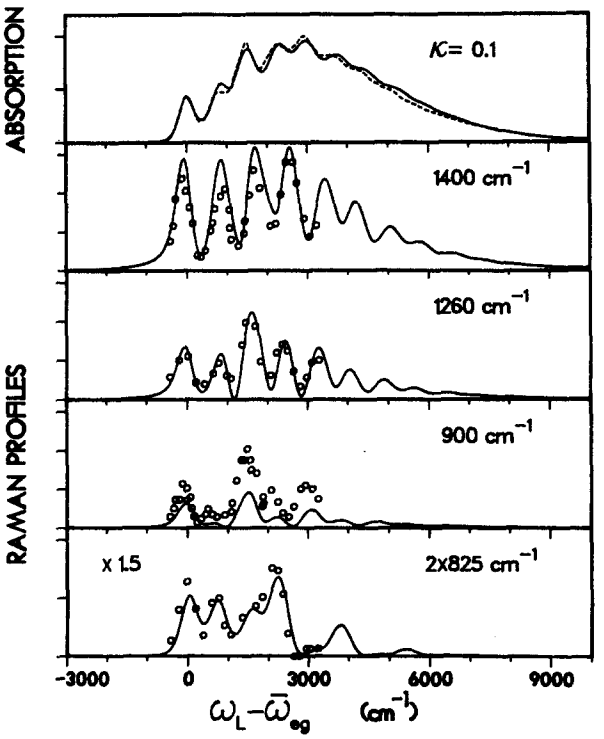


FIG. 4. Absorption and resonance Raman profiles for azulene in $CS_2$ at 300 K. The solid lines are theoretical curves computed using our seven-mode stochastic harmonic model without Dushinsky rotation. The absorption curve (upper panel) is $\omega_L \sigma(\omega_L)$ where $\sigma(\omega_L)$ is given in Appendix C. The dashed line is experimental [Ref. 8(b)]. The Raman profiles (lower four panels) were calculated in the rapid fluctuation limit using Eq. (34c) together with Eq. (57) and Eqs. (60)–(66). Shown are the experimental data [Ref. 8(b)] (circles) and the calculated profiles $|\chi_{ca}(\omega_L)|^2$ for four different Raman transitions as indicated in each panel. The structural parameters ($D_j$, $\omega_j'$, and $\omega_j''$) used in the calculation are given in Table I. The broadening parameters are $\Delta = 180$ cm$^{-1}$, $\Lambda = 18$ cm$^{-1}$, and $\Gamma_0 = 408$ cm$^{-1}$. $\gamma = 0$ and $\bar{\omega}_{eg} = 14\,286$ cm$^{-1}$.

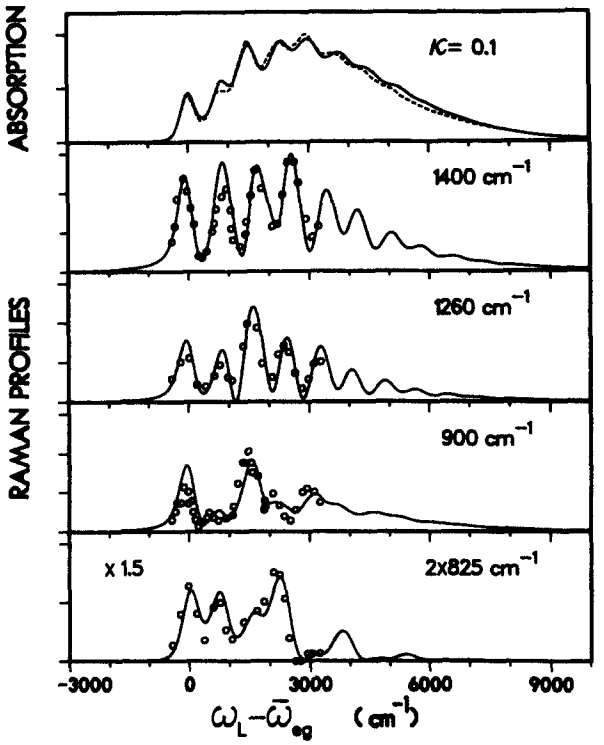


FIG. 5. The same as Fig. 4, except that we have included a $2\times2$ Dushinsky rotation matrix coupling the 900 and the 1400 cm$^{-1}$ modes. The off diagonal element $\bar{S}_{4,6}$ between these modes is $-0.25$. [Eq. (51)]. The Raman profiles were calculated using the equation of Appendix D for $G_{mn}(t)$ instead of Eqs. (60)–(66).

respects. First, the calculations of the Raman excitation profiles in Ref. 8(b) are perturbative in the displacements $D_j$; the present calculation uses the exact solution of the stochastic model and is nonperturbative. Second, we are using here a more general line-broadening mechanism with an arbitrary time scale for the solvent. Our best fit is displayed in Fig. 5. In Figs. 6 and 7 we demonstrate the dependence of our line shapes on $\kappa$. In these figures we kept the same structural parameters of Fig. 5 and varied $\kappa$ ($\kappa = 1, \infty$) keeping the FWHM of $J_0$ (i.e., $\Gamma_0$) fixed. The absorption and the Raman line shapes are not so sensitive to $\kappa$ as long as $\kappa \leqslant 0.1$. Had we used $\kappa = 0$ in Eq. (16) and still used Eqs. (34b), the fits would not be much different. This is illustrated by the solid line in Fig. 8. However, we should note that when $\kappa = 0$, we are in the static (inhomogeneous) limit, and Eq. (34b) should be replaced by Eq. (41). The solid line is therefore incorrect. Figure 8 shows also the resulting line shapes assuming inhomogeneous broadening ($\kappa = 0$) and using Eq. (41). The fit is obviously poor. We thus conclude that the broadening in this case is not inhomogeneous, although the absorption and the Raman profiles look pretty much Gaus-

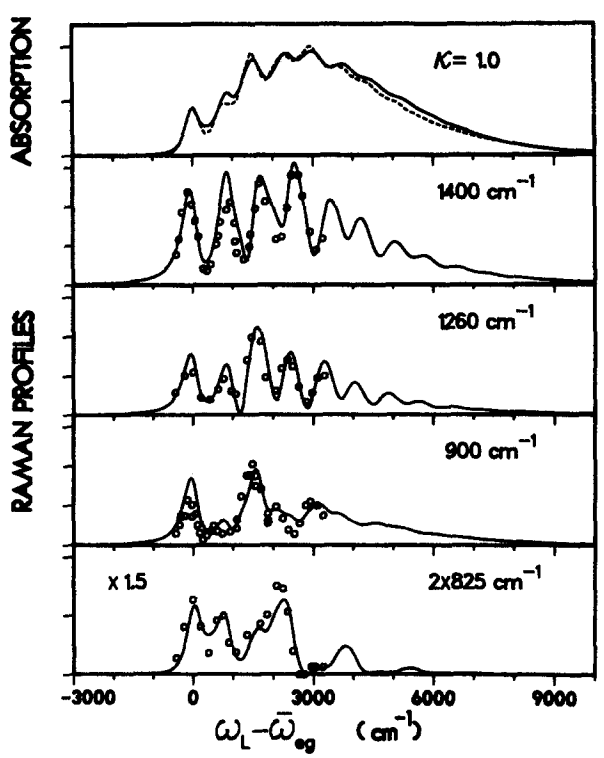


FIG. 6. The same as Fig. 5 but with different broadening parameters, $\Delta = 266$ cm$^{-1}$, $\Lambda = 266$ cm$^{-1}$, and $\Gamma_0 = 408$ cm$^{-1}$.



Downloaded 26 Jun 2002 to 128.151.176.185. Redistribution subject to AIP license or copyright, see http://ojps.aip.org/jcpo/jcpcr.jsp

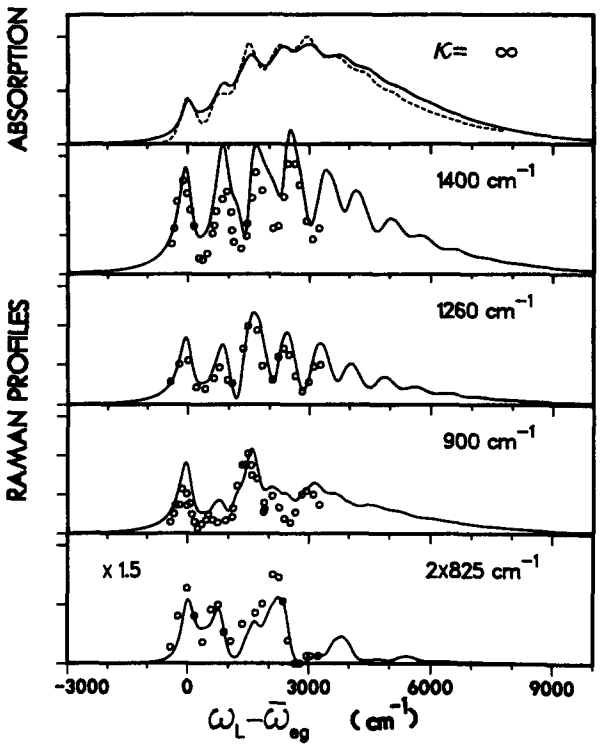


FIG. 7. The same as Fig. 5 with different broadening parameters corresponding to the fast modulation limit, $\kappa = \infty$, $\Gamma_0 = 2\Delta^2/\Lambda = 408\ \mathrm{cm}^{-1}$.

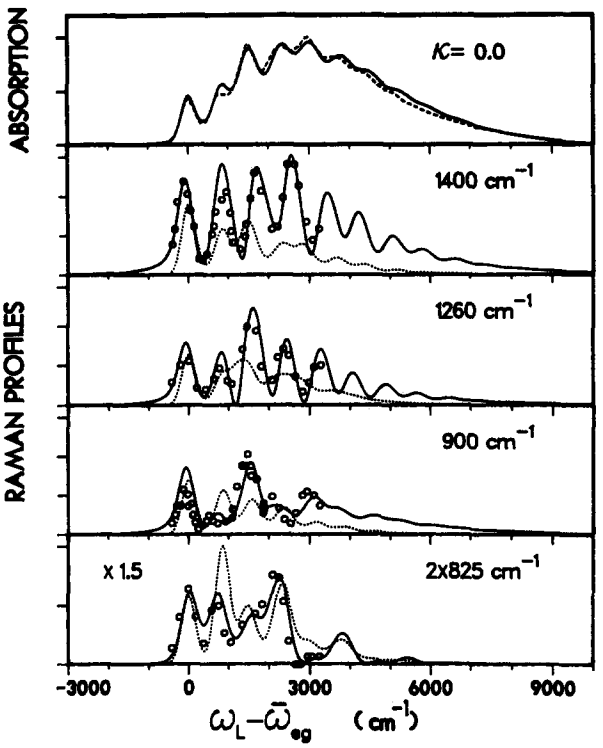


FIG. 8. The solid curves are the same as Fig. 5 with different broadening parameters corresponding to the static limit. We took $\Lambda = 0$, $\kappa = 0$, and $\Gamma_0 = 2.35\Delta = 408\ \mathrm{cm}^{-1}$. The fit is as good as that of Fig. 5 ($\kappa = 0.1$) since the absorption and the Raman profiles are not so sensitive to $\kappa$ for $\kappa \lesssim 0.1$. This calculation for the Raman profiles is, however, incorrect since in the static limit we cannot assume rapid fluctuation and Eq. (34a) should be replaced by Eqs. (40) or (41). The correct calculation for $\kappa = 0$ using Eq. (41) is the dotted curve and gives obviously a poor fit to the experimental data. This figure demonstrates that azulene in $CS_2$ is in the slow modulation but the rapid fluctuation limit, and it is important to keep $\Lambda$ (and $\kappa$) small but finite so that condition (32) holds, as in Fig. 5.

sian. In other words, the line broadening for azulene in $CS_2$ corresponds to the *rapid fluctuation but slow modulation* limit. In Ref. 8(b) the authors have calculated Eq. (34c) perturbatively in the nuclear displacements $D_j$ using a Gaussian broadening $g(\tau) = \Delta^2\tau^2/2$ with FWHM 353 $\mathrm{cm}^{-1}$. That broadening was obtained by postulating a bath of low frequency modes and making a short time approximation. It should be noted that this corresponds to our rapid fluctuation limit with $\kappa \ll 1$. The present analysis shows that it is essential to keep $\kappa$ finite, so that we are in the rapid fluctuation limit which allows us to use Eq. (34c). In Fig. 9 we display our fit for azulene in methanol. We have kept the same structural parameters of Fig. 5 and varied only the broadening parameters. Our fit results in $\Delta = 282\ \mathrm{cm}^{-1}$ and $\Lambda = 28\ \mathrm{cm}^{-1}$ corresponding to $\Gamma_0 = 640\ \mathrm{cm}^{-1}$ and $\kappa = 0.1$. For comparison, the FWHM of the Gaussian used in Ref. 8(b) to fit the same experimental data is 589 $\mathrm{cm}^{-1}$.

## VI. CONCLUDING REMARKS

The most significant result of the present article is the development of a stochastic theory for Raman line shapes which is valid for an arbitrary time scale of the bath. The existing theories of Raman line broadening in polyatomic molecules in solution consider only homogeneous (fast modulation) or inhomogeneous (static) broadening mechanisms. These correspond, respectively, to a bath characteristic time scale $\Lambda^{-1}$ which is very rapid or very slow, compared with the amplitude of modulation $\Delta$ of the electronic energy gap. The present theory is valid for any value of $\kappa = \Lambda/\Delta$. We have shown that the total emission rate $I(\omega_L,\omega_S) = I_1 + I_2 + I_3 + I_4$ [Eq. (28)] cannot, in general, be written as the square of an ensemble-averaged amplitude. We further considered the partitioning $I(\omega_L,\omega_S)$ into a Raman ($I_R$) and a fluorescence ($I_F$) component. This

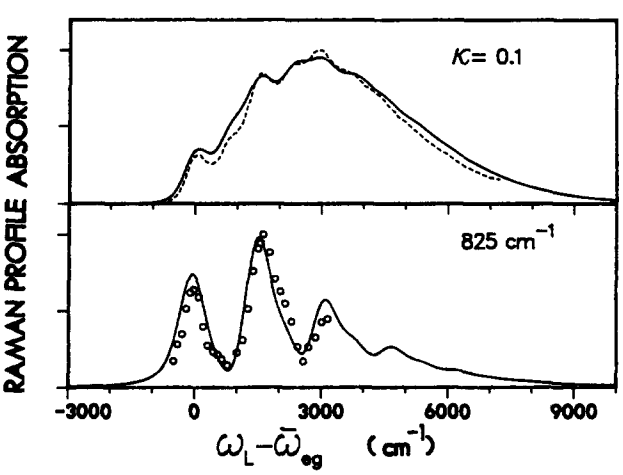


FIG. 9. Same as Fig. 5, except that the solvent is methanol [Ref. 8(b)] instead of $CS_2$. The broadening parameters are $\Delta = 282\ \mathrm{cm}^{-1}$, $\Lambda = 28\ \mathrm{cm}^{-1}$, and $\Gamma_0 = 640\ \mathrm{cm}^{-1}$. $\gamma = 0$ and $\bar{\omega}_{eg} = 14\,650\ \mathrm{cm}^{-1}$.



Downloaded 26 Jun 2002 to 128.151.176.185. Redistribution subject to AIP license or copyright, see http://ojps.aip.org/jcpo/jcpcr.jsp

separation depends on the various parameters in the problem and is not always unique. Equations (31), (34a), (37b), (41), or (46b) provide closed expressions for the Raman component for the various cases of line broadening. For the present discussion let us define the Raman yield ($Y_R$) and the fluorescence yield ($Y_F$) as follows:

$$Y_R(\omega_L) = \int \rho(\omega_s) I_R(\omega_L,\omega_S) d\omega_S/\sigma(\omega_L), \tag{70a}$$

$$Y_F(\omega_L) = \int \rho(\omega_s) I_F(\omega_L,\omega_S) d\omega_S/\sigma(\omega_L), \tag{70b}$$

where $\rho(\omega_s)$ is the density of modes of the radiation field.[42] Obviously, if all the lifetimes are radiative (no nonradiative decay channels), we have

$$Y_R + Y_F = 1. \tag{71}$$

$Y_R$ ($Y_F$) denote the number of Raman (fluorescence) photons emitted per $\omega_L$ photon absorbed. For an isolated molecule, in the absence of a thermal bath, we have $Y_R = 1$, all the emission is of the Raman-type, and $I_R$ can be written as an amplitude square resulting in the Kramers–Heisenberg formula [Eq. (1)]. The most common situation in solution is the rapid fluctuation case [Eq. (34)] in which the bath fluctuations are very rapid compared with the Raman linewidth ($\gamma_a + \gamma_c$). In this case, we have shown that the Raman excitation profiles can be written as the square of an ensemble-averaged amplitude. It should be reiterated that rapid fluctuation [Eq. (32)] does not imply fast modulation [Eq. 35)]. Within the rapid fluctuation limit $\kappa$ can be arbitrary and the absorption line shape can be homogeneous or very close to inhomogeneous. In the static limit ($\Lambda = 0$), however, we have to use Eq. (41), which results in the well-known formula for inhomogeneous broadening. We further showed that at large detunings the fluorescence disappears and $Y_R \to 1$. Our present fit to azulene shows that $\kappa \leqslant 0.1$, and that $\kappa \neq 0$. Apart from that, the absorption and Raman profiles are not so sensitive for $\kappa \lesssim 0.1$. Much more precise information regarding $\kappa$ is contained in the absolute yield $Y_R$ and its behavior with detuning of $\omega_L$. This yield will be analyzed in the future for other systems for which the absolute Raman cross section has been measured,[7] and will allow us to get more accurate estimates of the solvent parameters $\Delta$ and $\Lambda$.

## ACKNOWLEDGMENTS

The support of the National Science Foundation, the Office of Naval Research, the Army Research Office, and the Petroleum Research Fund, administered by the American Chemical Society, is gratefully acknowledged.

## APPENDIX A: THE PARTITIONING OF EQ. (28)

In this Appendix, we show how the partitioning of $I(\omega_L,\omega_S)$ [Eq. (28)] is obtained using the results of Ref. 20. [In Eqs. (27) and (47) of Ref. 20 $\phi^+(\tau_1,\tau_2,\tau_3)$ and $\Phi^-(\tau_1,\tau_2,\tau_3)$ should be interchanged. This is corrected in the following expressions.] In that article, the emission spectrum was expressed as a sum of three terms:

$$I(\omega_L,\omega_S) = \sum_{a,c} P(a) I_{ca}(\omega_L,\omega_S), \tag{A1}$$

where

$$I_{ca}(\omega_L,\omega_S) = K_{\rm I} + K_{\rm II} + K_{\rm III} \tag{A2}$$

and

$$K_I = -i \sum_{n=0}^{\infty} \sum_{bb'} \mu_{ab'}\mu_{b'c}\mu_{cb}\mu_{ba} \times \frac{(-1)^n}{\kappa^{2n} n!} \frac{J_n(\omega_L - \omega_{ba} + i\gamma/2)\, J_n(\omega_S - \omega_{bc} + i\gamma/2)}{\omega_{b'b} + i(\gamma + n\Lambda)} + \text{c.c.}, \tag{A3a}$$

$$K_{II} = -i \sum_{n=0}^{\infty} \sum_{bb'} \mu_{ab'}\mu_{b'c}\mu_{cb}\mu_{ba} \times \frac{1}{\kappa^{2n} n!} \frac{J_n(\omega_L - \omega_{ba} + i\gamma/2) J_n(\omega_{b'c} - \omega_S + i\gamma/2)}{\omega_{b'b} + i(\gamma + n\Lambda)} + \text{c.c.}, \tag{A3b}$$

$$K_{III} = -i \sum_{n=0}^{\infty} \sum_{bb'} \mu_{ab'}\mu_{b'c}\mu_{cb}\mu_{ba} \times \frac{1}{\kappa^{2n} n!} \frac{J_n(\omega_L - \omega_{ba} + i\gamma/2) J_n(\omega_{b'c} - \omega_S + i\gamma/2)}{\omega_L - \omega_S - \omega_{ca} + in\Lambda} + \text{c.c.} \tag{A3c}$$

Each of the three terms [Eqs. (A3)] correspond to a particular sequence of radiative interactions in Liouville space. It should be noted that $J_n(s)$ in this article [Eq. (17)] are defined slightly differently than in Ref. 20 [Eq. (C4)]. Here $s$ is a Fourier variable, whereas in Ref. 20, $s$ was a Laplace variable. The partitioning of Eqs. (A1)–(A3) in the form of Eq. (28) is obtained by making use of the identity

$$\frac{1}{\omega_L - \omega_S - \omega_{ca} + in\Lambda} = \frac{\omega_L - \omega_S - \omega_{ca}}{(\omega_L - \omega_S - \omega_{ca})^2 + (n\Lambda)^2} - \frac{in\Lambda}{(\omega_L - \omega_S - \omega_{ca})^2 + (n\Lambda)^2}. \tag{A4}$$

Upon the substitution of Eq. (A4) into Eq. (A3c), $K_{\rm III}$ is split into parts. The part containing the second term in Eq. (A4) with $n = 0$ results in $I_1$ [Eq. (28b)]. $I_2$ [Eq. (28c)] consists of the remaining $n > 0$ terms of this part. $I_4$ [Eq. (28e)] is given by the remaining part of $K_{\rm III}$, i.e., using the first term in Eq. (A4), and $I_3$ [Eq. (28d)] is given by $K_{\rm I} + K_{\rm II}$.



Downloaded 26 Jun 2002 to 128.151.176.185. Redistribution subject to AIP license or copyright, see http://ojps.aip.org/jcpo/jcpcr.jsp

## APPENDIX B: THE RAMAN EXCITATION PROFILES WITH INHOMOGENEOUS BROADENING

In this Appendix we show the equivalence of Eqs. (40) and (41). Upon the substitution of Eq. (40b) in Eq. (40a), we can carry out the summation over $n$ resulting in

$$I_R(\omega_L,\omega_S) = 2\pi\sum_{ac}\sum_{bb'}P(a)\mu_{ab}\mu_{b'a}\mu_{cb}\mu_{ba}\delta(\omega_L-\omega_S-\omega_{ca}) \times\int_0^\infty\int_0^\infty dt\,dt'\exp[-i(\omega_L-\omega_{ba})t - i(\omega_{b'a}-\omega_L)t' - \gamma/2(t+t') - \Delta^2(t-t')^2/2]. \quad (B1)$$

We now make use of the Fourier transform:

$$\exp(-\Delta^2\tau^2/2) = \frac{1}{\sqrt{2\pi}\Delta}\int_{-\infty}^{\infty}d\omega'\exp(i\omega'\tau-\omega'^2/2\Delta^2). \quad (B2)$$

Upon the substitution of Eq. (B2) into Eq. (B1) we can perform the integrations over $t$ and $t'$ resulting in

$$I_R(\omega_L,\omega_S) = \frac{\sqrt{2\pi}}{\Delta}\int_{-\infty}^{\infty}d\omega'\exp\left(\frac{-\omega'^2}{2\Delta^2}\right) \times\sum_{a,c}P(a)|\chi_{ca}(\omega_L-\omega')|^2 \times\delta(\omega_L-\omega_S-\omega_{ca}), \quad (B3a)$$

where

$$\chi_{ca}(\omega_L) = \sum_b\frac{\mu_{cb}\mu_{ba}}{\omega_L-\omega_{ba}+i\gamma/2}. \quad (B3b)$$

Equations (B3) are identical to Eq. (41).

## APPENDIX C: THE ABSORPTION LINE SHAPE FOR A GENERAL HARMONIC MOLECULE

In this Appendix we present the exact expressions for the absorption line shape of harmonic molecules characterized by the Hamiltonian [Eq. (47)]. The detailed derivation using Green function techniques was given in Refs. 40 and 41.

We first recast Eqs. (56) and (57), in the form

$$\sigma(\omega_L) = 2\,\mathrm{Re}\int_0^\infty dt\exp(i\omega_L t)\sigma(t)\exp[-g(t)]. \quad (C1)$$

For a polyatomic molecule at temperature $T$, $\sigma(t)$ may be written as[40,41]

$$\sigma(t) = |\psi(t)|^{-1/2}\exp[\mathbf{D}^T\mathsf{f}(t)\mathbf{D}], \quad (C2)$$

where $|\psi|$ denotes the determinant of the $\psi$ matrix. Here

$$\psi(t) = \tfrac{1}{4}(\mathsf{C}_+\mathsf{S}'\mathsf{A}_- + \mathsf{C}_-\mathsf{S}\mathsf{A}_+) \times(\mathsf{C}_+\mathsf{S}\mathsf{A}_- + \mathsf{C}_-\mathsf{S}'\mathsf{A}_+) \quad (C3)$$

and

$$\mathsf{f}(t) = -\mathsf{S}'\mathsf{A}_-(\mathsf{C}_+\mathsf{S}'\mathsf{A}_- + \mathsf{C}_-\mathsf{S}\mathsf{A}_+)^{-1}\mathsf{C}_-. \quad (C4)$$

The various $N\times N$ matrices appearing in these equations are

$$\mathsf{A}_\pm(t) = (\bar{n}+1) \pm \bar{n}\exp(i\omega''t), \quad (C5)$$

$$\mathsf{C}_\pm(t) = 1 \pm \exp(-i\omega' t), \quad (C6)$$

$$\bar{n} = [\exp(h\omega''/kT)-1]^{-1}, \quad (C7)$$

and

$$\mathsf{S}' = (\mathsf{S}^{-1})^T. \quad (C8)$$

$\omega$ are diagonal matrices with matrix elements

$$\omega''_{ij} = \omega''_i\delta_{ij}, \quad (C9)$$

$$\omega'_{ij} = \omega'_I\delta_{ij}. \quad (C10)$$

$\mathbf{D}^T$ and $(\mathsf{S}^{-1})^T$ denote the transpose of $\mathbf{D}$ and $\mathsf{S}^{-1}$, respectively. At zero temperature we have $\mathsf{A}_\pm = 1$ and $\bar{n} = 0$. In this case we denote $\sigma(t)$ by $\sigma_0(t)$. $\sigma_0(t)$ is used in Appendix D.

## APPENDIX D: THE RAMAN EXCITATION PROFILES IN THE PRESENCE OF DUSHINSKY ROTATION

The Raman excitation profile [Eq. (31) or Eq. (34a) or Eq. (37b) or Eq. (41) or Eq. (46b)] requires the evaluation of $\chi_{mn}(\omega_L)$ [Eq. (57)]. The key quantity in Eq. (57) is the Green function $G_{mn}(t)$, which may be recast in the form

$$G_{mn}(t) = G_{00}(t)W_{mn}(t), \quad (D1)$$

where $G_{00}(t) = \sigma_0(t)$, which is given in Eq. (C2) at $T=0$ K. It is defined in Appendix C by setting $\bar{n}=0$ (or $\mathsf{A}_\pm = 1$).

The most general expression of $W_{mn}(t)$ is presented elsewhere.[41] In most cases, the experimental spectra only involve exciting one of the modes, say, mode $j$ (e.g., the resonance Raman spectra for azulene[8]). In this case, $|\mathbf{m}\rangle = |0,...,m,...,0\rangle$ and $|\mathbf{n}\rangle = |0,...,n,...,0\rangle$. The $j$'th mode changes from state $n$ to $m$, all the other modes are in the ground state. In this case we have[41]

$$W_{mn}(t) = (m!n!2^{m+n})^{-1/2} \times\sum_{p=0}^{m}\sum_{q=0}^{n}(-1)^p\binom{m}{p}\binom{n}{q}[\alpha(t)]^{m+n-p-q} \times[\tilde{\alpha}(t)]^{p+q}\cdot H_{m+n-p-q} \times[\zeta(t)/\alpha(t)]H_{p+q}(0), \quad (D2)$$

where

$$\alpha(t) = \{1/2 - [(\mathsf{C}_+\mathsf{S}'+\mathsf{C}_-\mathsf{S})^{-1}\mathsf{C}_+\mathsf{S}']_{jj}\}^{1/2}, \quad (D3)$$

$$\tilde{\alpha}(t) = \{1/2 - [(\mathsf{C}_+\mathsf{S}+\mathsf{C}_-\mathsf{S}')^{-1}\mathsf{C}_-\mathsf{S}']_{jj}\}^{1/2}, \quad (D4)$$

and

$$\zeta(t) = [-(\mathsf{C}_+\mathsf{S}'+\mathsf{C}_-\mathsf{S})^{-1}\mathsf{C}_-\mathbf{D}]_j = [\mathsf{S}^T\mathsf{f}(t)\mathbf{D}]_j. \quad (D5)$$

When $n=0$, Eq. (D2) assumes the form

$$W_{m0}(t) = (m!2^m)^{-1/2}[\beta(t)]^m H_m[\zeta(t)/\beta(t)], \quad (D6)$$

where

$$\beta(t) = [\alpha^2(t)+\tilde{\alpha}^2(t)]^{1/2}. \quad (D7)$$

When $m=1$, Eq. (D6) further reduces to

$$W_{10}(t) = 2^{1/2}\zeta(t). \quad (D8)$$

In the absence of mode mixing, i.e., when the Dushinsky transformation matrix $\mathsf{S}$ (or $\overline{\mathsf{S}}$) is diagonal, these equations reduce to Eqs. (61)–(68).



Downloaded 26 Jun 2002 to 128.151.176.185. Redistribution subject to AIP license or copyright, see http://ojps.aip.org/jcpo/jcpcr.jsp

[1]J. Tang and A. C. Albrecht, in *Raman Spectroscopy*, edited by H. A. Szymanski (Plenum, New York, 1970), Vol. 2, p. 33; P. M. Champion and A. C. Albrecht, Annu. Rev. Phys. Chem. **333**, 353 (1982).
[2]B. R. Stallard, P. M. Champion, P. R. Collis, and A. C. Albrecht, J. Chem. Phys. **78**, 712 (1983); D. Lee, B. R. Stallard, P. M. Champion, and A. C. Albrecht, J. Phys. Chem. **88**, 6693 (1984).
[3]B. Johnson and W. Peticolas, Annu. Rev. Phys. Chem. **27**, 465 (1976); L. Chinsky, A. Laigle, W. L. Peticolas, and P. Y. Turpin, J. Chem. Phys. **76**, 1 (1982).
[4]T. G. Spiro, Adv. Protein Chem. **37**, 111 (1985).
[5]Z. Z. Ho, R. C. Hanson, and S. H. Lin, J. Chem. Phys. **77**, 3414 (1982); Z. Z. Ho, T. A. Moore, S. H. Lin, and R. C. Hanson, *ibid.* **74**, 873 (1981); Z. Z. Ho, R. C. Hanson, and S. H. Lin, J. Phys. Chem. **89**, 1014 (1985).
[6]W. Siebrand and Z. Zgierski, J. Chem. Phys. **71**, 3561 (1979); in *Excited States*, edited by E. C. Lim (Academic, New York, 1979), Vol. 4, Part 1; W. Siebrand and M. Z. Zgierski, J. Chem. Phys. **71**, 3561 (1979).
[7]A. B. Myers, R. A. Harris, and R. A. Mathies, J. Chem. Phys. **79**, 603 (1983); A. B. Myers, M. O. Trulson, and R. A. Mathies, *ibid.* **83**, 5000 (1985); A. B. Myers, M. O. Trulson, J. A. Pardoen, C. Heeremans, J. Lugtenburg, and R. A. Mathies, *ibid.* **84**, 633 (1986); A. B. Myers and R. A. Mathies, in *Biological Applications of Raman Spectroscopy* (to be published).
[8](a) O. Brafman, C. K. Chan, B. Khodadoost, J. B. Page, and C. T. Walker, J. Chem. Phys. **80**, 5406 (1984); (b) C. K. Chan, J. B. Page, D. L. Tonks, O. Brafman, B. Khodadoost, and C. T. Walker, *ibid.* **82**, 4813 (1985).
[9]F. Inagaki, M. Tasumi, and T. Miyazawa, J. Mol. Spectrosc. **50**, 286 (1974); S. Saito, M. Tasumi, and C. H. Eugster, J. Raman Spectrosc. **14**, 299 (1983); S. Saito and M. Tasumi, *ibid.* **14**, 310 (1983).
[10]J. B. Page and D. L. Tonks, J. Chem. Phys. **75**, 5694 (1981); C. K. Chan and J. B. Page, *ibid.* **79**, 5234 (1983); Chem. Phys. Lett. **104**, 609 (1984).
[11]T. Kitagawa, M. Abe, and H. Ogoshi, J. Chem. Phys. **69**, 4516 (1978); M. Abe, T. Kitagawa, and Y. Kyogoku, *ibid.* **69**, 4526 (1978).
[12]B. E. Kohler, T. A. Spiglanin, R. J. Hemley, and M. Karplus, J. Chem. Phys. **80**, 23 (1984); J. R. Ackerman, S. A. Forman, H. Hossain, and B. E. Kohler, *ibid.* **80**, 39 (1984).
[13]A. Warshel, Annu. Rev. Biophys. Bioeng. **6**, 273 (1977); A. Warshel and P. Dauber, J. Chem. Phys. **66**, 5477 (1977).
[14]B. S. Hudson, B. E. Kohler, and K. Schulten, in *Excited States*, edited by E. C. Lim (Academic, New York, 1982).
[15]R. R. Langridge-Smith, D. V. Brumbaugh, C. A. Hoyman, and D. H. Levy, J. Phys. Chem. **85**, 3742 (1981).
[16]C. S. Parmenter, J. Phys. Chem. **86**, 1735 (1982).
[17]V. E. Bondybey, Annu. Rev. Phys. Chem. **35**, 591 (1984).
[18]W. R. Lambert, P. M. Felker, and A. H. Zewail, J. Chem. Phys. **75**, 5958 (1981).
[19]D. G. Leopold, V. Vaida, and M. F. Granville, J. Chem. Phys. **81**, 4210 (1984); D. G. Leopold, R. D. Pendley, J. L. Roebber, R. J. Hemley, and V. Vaida, *ibid.* **81**, 4218 (1984); V. Vaida, Acc. Chem. Res. (in press).
[20]S. Mukamel, J. Chem. Phys. **82**, 5398 (1985).
[21]S. Mukamel, J. Chem. Phys. **71**, 2884 (1979); S. Mukamel and R. E. Smalley, *ibid.* **73**, 4156 (1980).
[22]S. Mukamel, J. Phys. Chem. **89**, 1077 (1985); J. Chem. Phys. **82**, 2867 (1985).
[23]H. A. Kramers and W. Heisenberg, Z. Phys. **31**, 681 (1925).
[24]D. L. Huber, Phys. Rev. **170**, 418 (1968); **178**, 93 (1969); **187**, 392 (1969).
[25]A. Omont, E. W. Smith, and J. Cooper, Astrophys. J. **175**, 185 (1972).
[26]P. F. Liao, J. E. Bjorkholm, and P. R. Berman, Phys. Rev. A **20**, 1489 (1977); J. L. Carlsten, A. Szoke, and M. G. Raymer, *ibid.* **15**, 1029 (1977).
[27]S. Mukamel and J. Jortner, in *Excited States*, edited by E. C. Lim (Academic, New York, 1977), Vol. 3; S. Mukamel, A. Ben Reuven, and J. Jortner, Phys. Rev. A **12**, 947 (1975).
[28]J. M. Friedman and R. M. Hochstrasser, Chem. Phys. Lett. **33**, 225 (1975); Chem. Phys. **6**, 155 (1974).
[29]S. Mukamel, Phys. Rep. **93**, 1 (1982).
[30]K. Burnett, Phys. Rep. **118**, 339 (1985).
[31]Y. R. Shen, Phys. Rev. B **9**, 622 (1974).
[32]R. M. Hochstrasser and C. A. Nyi, J. Chem. Phys. **70**, 1112 (1979).
[33]Y. Toyozawa, J. Phys. Soc. Jpn. **41**, 400 (1976); A. Kotani and Y. Toyozawa, *ibid.* **41**, 1699 (1976).
[34]T. Takagahara, E. Hanamura, and R. Kubo, J. Phys. Soc. Jpn. **43**, 802, 811, 1522 (1977); **44**, 728, 742 (1978); R. Kubo, T. Takagahara, and E. Hanamura, Solid State Commun. **32**, 1 (1979).
[35]J. Sue and S. Mukamel (to be published).
[36]S. Hassing and O. S. Mortensen, J. Chem. Phys. **73**, 1078 (1980).
[37]N. Bloembergen, E. M. Purcell, and R. V. Pound, Phys. Rev. **73**, 679 (1948).
[38]P. W. Anderson and P. R. Weiss, Rev. Mod. Phys. **25**, 269 (1953).
[39]R. Kubo, Adv. Chem. Phys. **15**, 101 (1969).
[40]S. Mukamel, S. Abe, Y. J. Yan, and R. Islampour, J. Phys. Chem. **89**, 201 (1985).
[41]Y. Yan and S. Mukamel (to be published).
[42]W. H. Louisell, *Quantum Statistical Properties of Radiation* (Wiley, New York, 1973).



Downloaded 26 Jun 2002 to 128.151.176.185. Redistribution subject to AIP license or copyright, see http://ojps.aip.org/jcpo/jcpcr.jsp